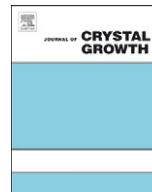




ELSEVIER

Contents lists available at ScienceDirect

## Journal of Crystal Growth

journal homepage: [www.elsevier.com/locate/jcrysgro](http://www.elsevier.com/locate/jcrysgro)

# Epitaxial growth of Cu<sub>2</sub>O and ZnO/Cu<sub>2</sub>O thin films on MgO by plasma-assisted molecular beam epitaxy

Davis S. Darvish\*, Harry A. Atwater

Thomas J. Watson Laboratory of Applied Physics, California Institute of Technology, Pasadena, CA 91125, USA

## ARTICLE INFO

### Article history:

Received 13 December 2010

Received in revised form

14 January 2011

Accepted 24 January 2011

Communicated by K.H. Ploog

Available online 1 February 2011

### Keywords:

A3. Molecular beam epitaxy

B1. Oxides

B2. Semiconducting materials

B3. Heterojunction semiconductor device

solar cell

## ABSTRACT

We report the epitaxial growth of Cu<sub>2</sub>O (0 0 1) and *m*-plane (1 0  $\bar{1}$  0) ZnO/Cu<sub>2</sub>O thin films on both bulk MgO (0 0 1) and biaxially textured thin films of MgO (0 0 1) via plasma-assisted molecular beam epitaxy. Cube on cube epitaxial growth of Cu<sub>2</sub>O thin films on both bulk MgO (0 0 1) and biaxially textured thin films of MgO (0 0 1) was observed and confirmed via X-ray diffraction and reflection high energy electron diffraction measurements. In addition, epitaxial *m*-plane ZnO growth via plasma-assisted MBE was conducted on both MgO substrates and Cu<sub>2</sub>O/MgO substrates. The ability to grow oriented, high-quality n-ZnO/p-Cu<sub>2</sub>O heterostructures enables improved thin film morphology and may have important implications for optoelectronic and photovoltaic devices.

© 2011 Elsevier B.V. All rights reserved.

## 1. Introduction

Cuprous oxide (Cu<sub>2</sub>O) is a non-toxic semiconductor with a direct band gap of 2.17 eV [1], which is potentially useful for photovoltaic cells and photo-electrolysis of water. It has been reported to have a long minority carrier diffusion length ( $\sim 5 \mu\text{m}$ ) [2], and is also composed of both earth-abundant and inexpensive elements [3]. Cuprous oxide is typically a p-type semiconductor due to intrinsic doping by copper vacancies, and efforts to form high-quality homojunctions by n-doping of Cu<sub>2</sub>O have largely been unsuccessful. However recent reports include n-type doping of Cu<sub>2</sub>O films grown by electrodeposition [4], and homojunctions with reported 200 mV open circuit voltages [5], but the source of n-type doping and voltage remain controversial [6]. Consequently, photovoltaic devices employing Cu<sub>2</sub>O are likely to use either the Schottky barriers or the semiconductor heterojunctions as a means for charge carrier separation. The approach taken in this paper anticipates the use of n-ZnO as the heterojunction partner for p-Cu<sub>2</sub>O in photovoltaic devices. There have been many reports on Cu<sub>2</sub>O solar cells prepared by various techniques, including electrodeposition [3], thermal oxidation of copper sheets [7], and sputter deposition [8]. However, the energy conversion efficiencies of these cells were only a fraction of their respective Shockley–Queisser theoretical values. To date, Cu<sub>2</sub>O

p–n heterojunctions have not demonstrated good photovoltaic performance, but in most of the previous investigations of Cu<sub>2</sub>O thin film growth, film orientation and microstructure were not well controlled. The lack of high-quality heterojunction interfaces between Cu<sub>2</sub>O and ZnO reduced the open circuit voltage and fill factor, resulting in a record efficiency of only 2% [9].

In this paper, we investigate the growth of epitaxial MgO, Cu<sub>2</sub>O, and ZnO by molecular beam epitaxy in order to better understand and control the heterostructure properties. *In situ* characterization of film structure and orientation was performed using reflection high energy electron diffraction (RHEED). Further post-growth structural analysis was performed via X-ray diffraction  $\omega - 2\theta$  and rocking curve measurements using Cu K <sub>$\alpha$</sub>  radiation.

## 2. Experimental

Plasma-assisted molecular beam epitaxy (MBE) was used for the fabrication of Cu<sub>2</sub>O thin films, as it provided control over critical growth conditions such as temperature, flux, base pressure, and interface sharpness. We used two types of substrates for film growth: cubic single crystal magnesium oxide MgO (0 0 1) and biaxially textured thin films of MgO/SiO<sub>2</sub>/Si grown by ion beam-assisted deposition (IBAD) [10]. The IBAD method allows the formation of MgO templates on inexpensive substrates, and could allow the growth of a tandem structure comprised of a Cu<sub>2</sub>O thin film cell on top of a solar cell fabricated on a bulk wafer

\* Corresponding author.

E-mail address: [ddarvish@caltech.edu](mailto:ddarvish@caltech.edu) (D.S. Darvish).

substrate (e.g., Si bottom cell). For bulk MgO substrates there is a lattice mismatch of only 1.1% between  $\text{Cu}_2\text{O}$  ( $a=0.427$  nm) and MgO ( $a=0.422$  nm), which facilitated epitaxial growth. In MBE growth, a copper effusion cell was operated with a beam equivalent

pressure of  $5 \times 10^{-7}$  Torr in the presence of a RF oxygen plasma ( $P=300$  W) at  $10^{-6}$  Torr, which resulted in a deposition rate of .025 nm/s. MgO substrates were annealed for 1 hour at  $T=650$  °C with varying partial pressures of oxygen in the range

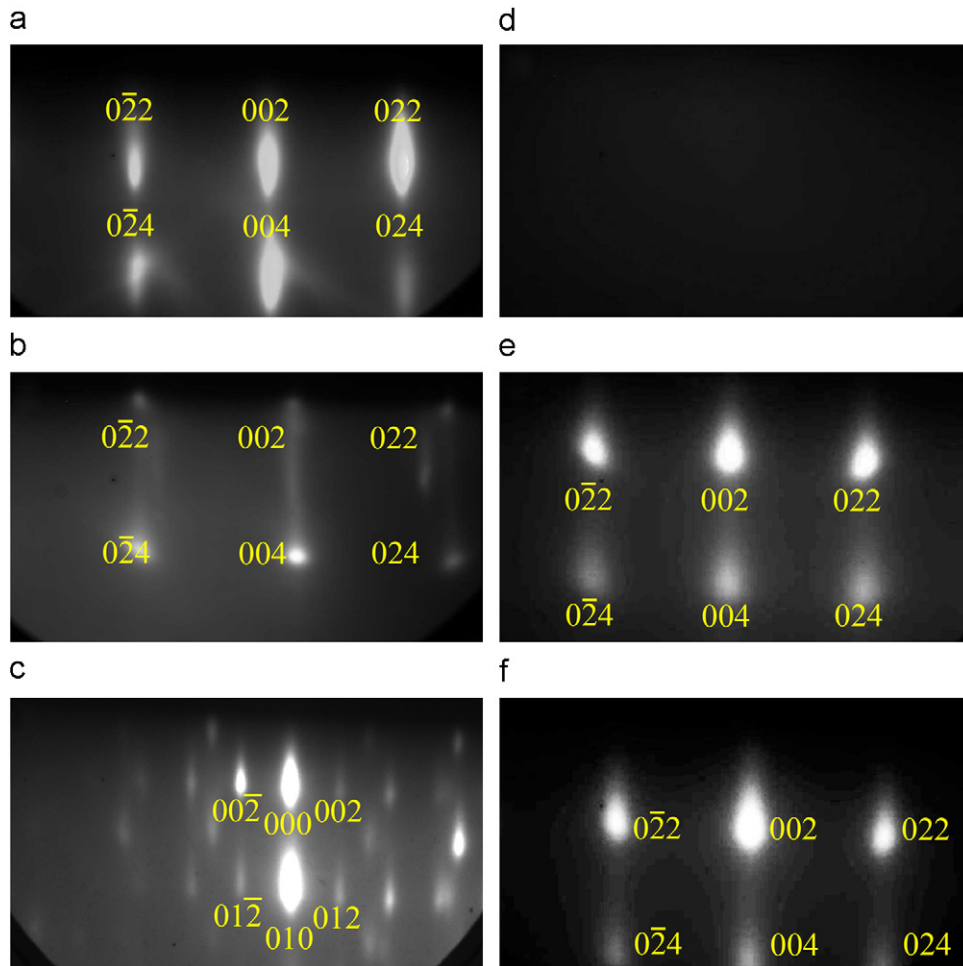


**Fig. 1.** *In situ* RHEED images from a clean MgO(0 0 1) substrate (a) followed by the deposition of a 70 nm  $\text{Cu}_2\text{O}$  film (b) and 70 nm *m*-plane ZnO on top of the  $\text{Cu}_2\text{O}$  layer are shown on the right hand column. *In situ* RHEED images of a clean  $\text{SiO}_2$  surface (d) followed by 10 nm deposition of IBAD MgO(0 0 1) (e) and 70 nm of  $\text{Cu}_2\text{O}$  (f) are shown on the left hand column.

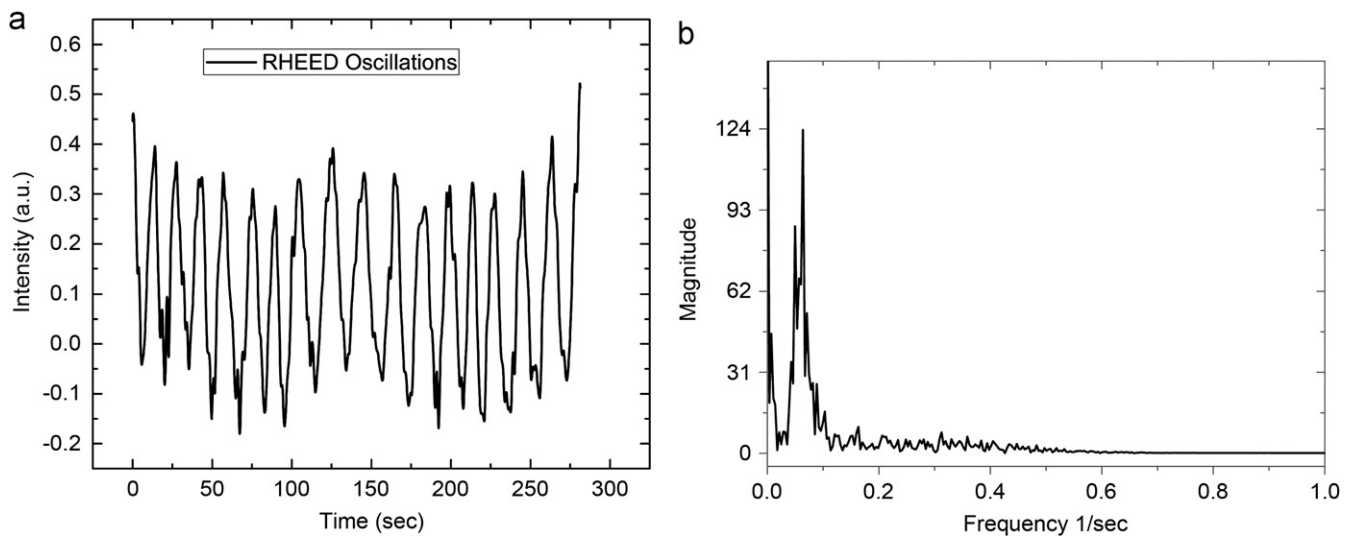


**Fig. 2.** (a) RHEED oscillations demonstrating layer-by-layer epitaxial growth of  $\text{Cu}_2\text{O}$  on MgO. (b) Fourier transform of RHEED oscillations to determine growth rate.

$P_{O_2} = 10^{-4} - 10^{-6}$  Torr, where a pressure  $P_{O_2} = 10^{-6}$  Torr provided the sharpest RHEED patterns.

Ion beam-assisted deposition of biaxially textured MgO (0 0 1) on amorphous  $SiO_2$  was conducted and film orientation was confirmed via RHEED, as illustrated in Fig. 1. IBAD was executed as a three-phase process where a 750 eV  $Ar^+$  ion beam was directed toward an amorphous substrate at a  $45^\circ$  angle for the

deposition of MgO by e-beam evaporation. During the first phase, an amorphous MgO film less than 4 nm thickness was deposited. During the second phase of growth, MgO crystals nucleated via solid phase crystallization with out-of-plane texturing. In the third stage of growth, in-plane texturing was evolved due to the amorphization of grains with misaligned in-plane texturing from the  $Ar^+$  ions. The  $Ar^+$  ions channeled in the (0 1 1) direction and

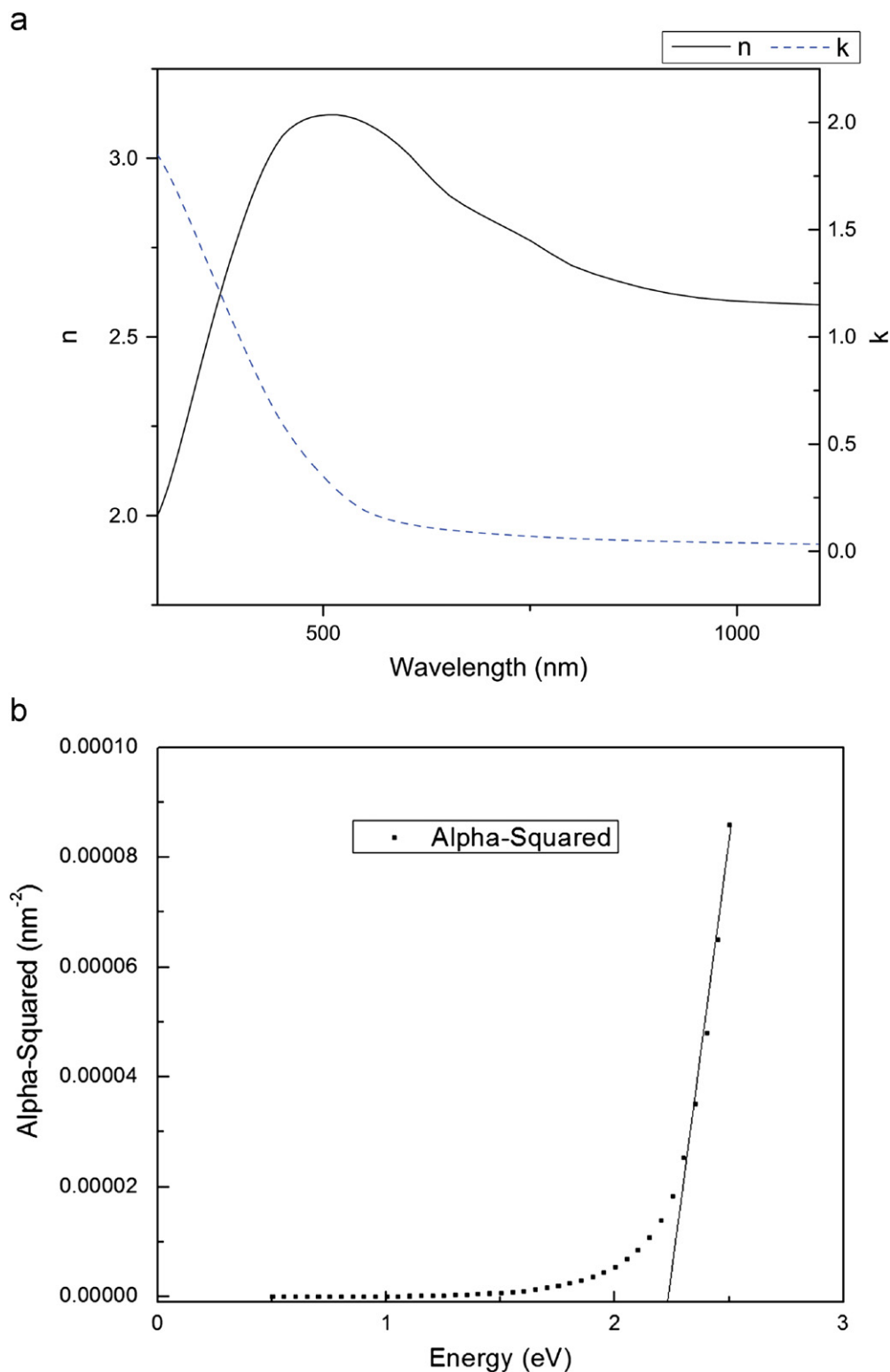


**Fig. 3.** Spectroscopic ellipsometry data for real and imaginary index of refraction for  $Cu_2O$  (70 nm) thin film. Inset shows alpha squared vs. energy, which allows extrapolation of band gap of  $Cu_2O$  to approximately 2.2 eV.

amorphized the grains that were not in the (0 0 1) direction. When a sufficiently thick MgO film was deposited, a (0 0 1) MgO film texture was formed as a result of a competitive amorphization process in which  $\text{Ar}^+$  ion channeling along [1 1 0] directions minimizes damage for the (0 0 1) film orientation but amorphizes grains with other orientations. This  $\text{Ar}^+$  ion beam was then turned off after 10 nm of growth and epitaxial MgO was deposited at an elevated substrate temperature to create a reduced defect density MgO (0 0 1) substrate template. It was then possible to grow  $\text{Cu}_2\text{O}$  with microstructure and properties similar to films grown on bulk MgO substrates.

We used thermally oxidized silicon wafers with a  $1\ \mu\text{m}$  amorphous  $\text{SiO}_2$  layer as starting substrates for IBAD growth. Using e-beam evaporation, thin films of MgO were deposited at room temperature on our  $\text{SiO}_2$  substrates at a rate of 0.2 nm/s with simultaneous ion bombardment by 750 eV  $\text{Ar}^+$  ions from a

Kaufman source ion gun until the MgO film thickness reached approximately 10 nm. A second electron-beam evaporation step was conducted at an elevated substrate temperature without the ion beam to produce a higher quality MgO film. The surface morphology and its evolution during growth of the biaxially textured MgO films were monitored using RHEED analysis. The second MgO deposition step added approximately 5 nm of MgO for a total MgO thickness of 15 nm in the biaxially textured template substrate.

ZnO thin films were grown (growth rate of 0.2 nm/s) on MgO (0 0 1) substrates and on  $\text{Cu}_2\text{O}$  (0 0 1)/MgO (0 0 1) substrates by MBE using a zinc effusion cell and a RF oxygen plasma. Prior to the ZnO growth, the substrates were thermally cleaned at  $T=450\ ^\circ\text{C}$  in the presence of the oxygen plasma for 15 min. ZnO was then grown at a substrate temperature  $T=350\ ^\circ\text{C}$  in the presence of a RF oxygen plasma ( $P=200\ \text{W}$ ) at  $5 \times 10^{-5}$  Torr with

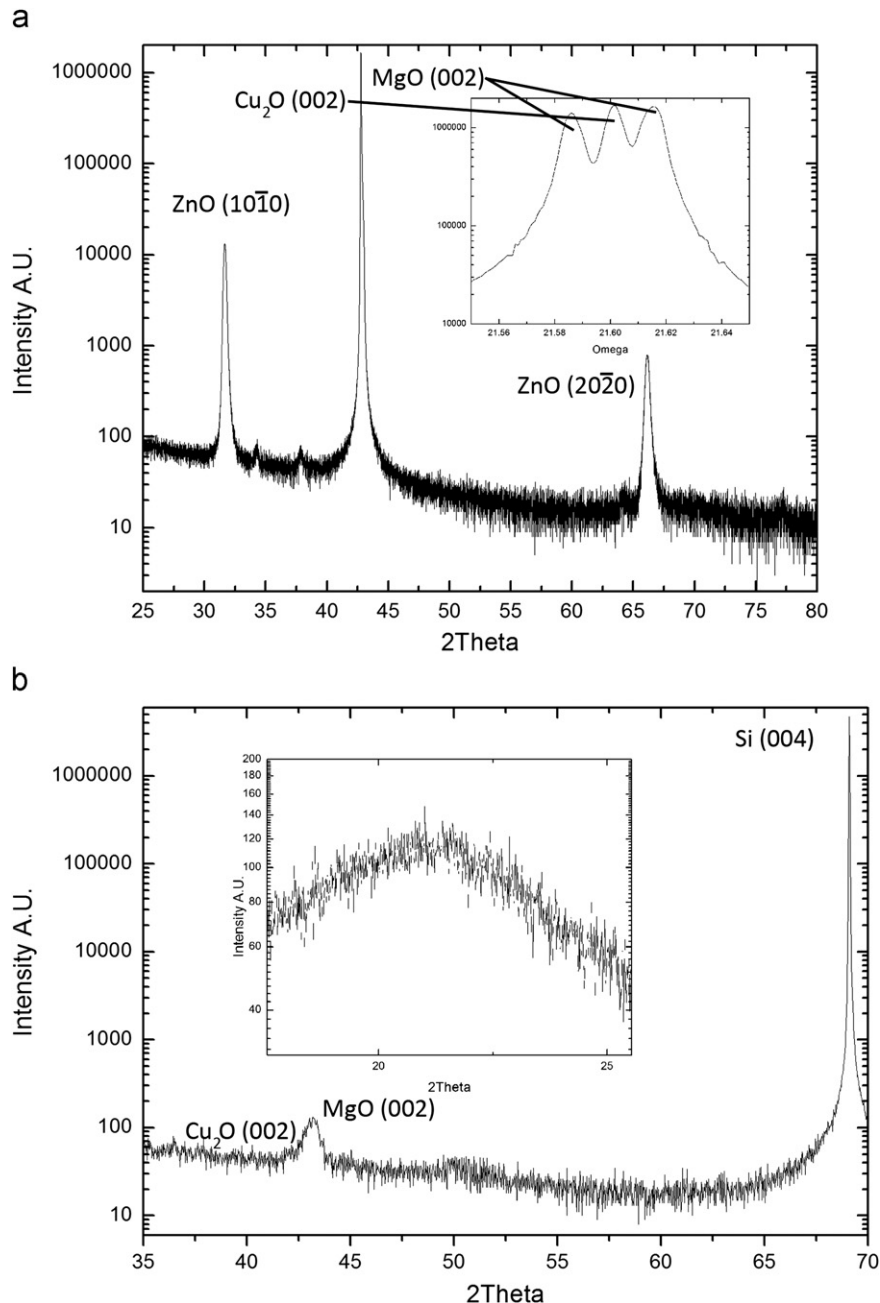


**Fig. 4.** (a)  $\omega$ - $2\theta$  X-ray scan of  $(1\ 0\ \bar{1}\ 0)$  ZnO (70 nm)/(0 0 2)  $\text{Cu}_2\text{O}$  (70 nm)/(0 0 2) MgO with  $\omega$  rocking curve of (0 0 2)  $\text{Cu}_2\text{O}$  on (0 0 2) MgO peak. (b)  $\omega$ - $2\theta$  X-ray scan of (0 0 2)  $\text{Cu}_2\text{O}$  (70 nm) on (0 0 2) IBAD MgO (10 nm) grown on an oxidized silicon substrate with  $\omega$  rocking curve of (0 0 2)  $\text{Cu}_2\text{O}$  on (0 0 2) MgO peak.

a Zn beam equivalent pressure of  $10^{-6}$  Torr. The growth rate of 0.2 nm/s was critical in obtaining the *m*-plane (1 0  $\bar{1}$  0) orientation of ZnO as opposed to the typically observed *c*-plane (0 0 0 1) orientation.

### 3. Results and discussion

Both the MgO substrate and Cu<sub>2</sub>O film exhibited a cubic crystal structure and closely matched lattice parameters. Cube on cube epitaxy of Cu<sub>2</sub>O (0 0 1) was observed on MgO (0 0 1) ( $T_{sub}=650$  °C, RF oxygen plasma ( $P=300$  W) at  $10^{-6}$  Torr, Cu BEP  $5 \times 10^{-7}$  Torr), and *in situ* RHEED was used to confirm the epitaxial growth, as illustrated in Fig. 1. The thickness of the layers was 70 nm for both the Cu<sub>2</sub>O and ZnO. The observed RHEED oscillations, shown in Fig. 2, indicated layer-by-layer growth of the Cu<sub>2</sub>O film in a two-dimensional island nucleation regime. For Cu<sub>2</sub>O (0 0 1)/MgO (0 0 1) epitaxy was observed in the temperature range of  $T_{sub}=550$ – $650$  °C, and RHEED oscillations were typically seen if growth of the film could be well controlled and grown slowly (approximately 0.2 Å/s). The streaky nature of the RHEED images indicated that the Cu<sub>2</sub>O films were relatively smooth. The surface roughness of the film slightly increased as a function of the film thickness, evident by the fading intensity of the RHEED pattern. A one-hour anneal at  $T_{sub}=650$  °C and  $P_{O_2}=10^{-6}$  Torr restored a great deal of the intensity and decreased the surface roughness. X-ray diffraction data illustrated in Fig. 4 confirmed the (0 0 1) Cu<sub>2</sub>O orientation and rocking curve analysis showed epitaxial growth of Cu<sub>2</sub>O on MgO with (0 0 1) peaks at  $\omega=21.58^\circ$  and  $21.61^\circ$  for Cu<sub>2</sub>O and MgO, respectively.

In addition to structural properties, the electronic and optical properties of Cu<sub>2</sub>O films were also characterized. Hall measurements showed hole mobilities in the range of 50–70 cm<sup>2</sup>/V s and hole concentrations in the range of  $10^{16}$ /cm<sup>3</sup>, which is dependent on substrate temperature history and oxygen plasma partial pressure during Cu<sub>2</sub>O film growth and cool-down. Spectroscopic ellipsometry was performed at an angle of incidence of 50°, 60°, and 70° for  $300 < \lambda < 850$  nm with a Xe lamp visible light source. The  $\psi(\omega), \Delta(\omega)$  data were converted to the  $n(\omega), k(\omega)$  values in Fig. 3(a), assuming bulk-like isotropic Cu<sub>2</sub>O films on MgO (0 0 1) substrates. Using the ellipsometry measurements, we were also able to extrapolate the energy band gap of the Cu<sub>2</sub>O film to 2.2 eV, shown in Fig. 3(b), which agrees with previously reported studies [8].

MgO substrates were also used for the growth of ZnO by oxygen plasma-assisted MBE. On nucleation of the film, the RHEED patterns illustrated in Fig. 1 transitioned from a streaky to a spotty pattern, indicating a single predominant orientation of growth. The crystalline orientations as determined by analysis of both the RHEED pattern (Fig. 1) and XRD (Fig. 4) showed a

preferential orientation of ZnO in the (1 0  $\bar{1}$  0) direction. The (1 0  $\bar{1}$  0) peak corresponds to the *m*-plane of ZnO. Similar results were obtained when growing ZnO on Cu<sub>2</sub>O thin films that were grown on MgO.

### 4. Conclusion

We have achieved epitaxial growth of Cu<sub>2</sub>O and ZnO on both single crystal (0 0 1) MgO and (0 0 1) IBAD MgO substrates. MBE growth of the Cu<sub>2</sub>O/ZnO heterojunction enabled a high degree of control over crystal orientation and interface quality. Structural, optical, and electrical qualities of the film were characterized using RHEED, X-ray diffraction, spectroscopic ellipsometry, and Hall measurements. These measurements confirmed the high morphological and electrical quality of epitaxially grown Cu<sub>2</sub>O films. We have also successfully demonstrated MBE growth of epitaxial ZnO on (1 0  $\bar{1}$  0) bulk MgO (0 0 1) and on Cu<sub>2</sub>O (0 0 1) films.

### Acknowledgment

This work was supported by the Office of Energy Efficiency and Renewable Energy, U.S. Department of Energy, under Grant DE-FG36-08GO18006 and Dow Chemical Company.

### References

- [1] T. Minami, T. Miyata, K. Ihara, Y. Minamino, S. Tsukada, Effect of ZnO film deposition methods on the photovoltaic properties of ZnO–Cu<sub>2</sub>O heterojunction devices, *Thin Solid Films* (2006) 47–52.
- [2] C.A. Dimitriadis, L. Papadimitriou, N.A. Economou, Resistivity dependence of minority carrier diffusion length in single crystals of Cu<sub>2</sub>O, *J. Mater. Sci. Lett.* (1983) 691–693.
- [3] S. Ishizuka, K. Suzuki, Y. Okamoto, M. Yanagita, T. Sakurai, K. Akimoto, N. Fujiwara, H. Kobayashi, K. Matsubara, S. Niki, Polycrystalline n-ZnO/p-Cu<sub>2</sub>O heterojunctions grown by RF-magnetron sputtering, *Phys. Status Solidi* (1996) 399.
- [4] K. Han, M. Tao, Electrochemically deposited p–n homojunctions cuprous oxide solar cells, *Sol. Energy Mater. Sol. Cells* (2009) 153–157.
- [5] D. Scanlon, G. Watson, Undoped n-Type Cu<sub>2</sub>O: Fact or Fiction?, *J. Phys. Chem. Lett.* (2010) 2582–2585.
- [6] C. McShane, Effect of junction morphology on the performance of polycrystalline Cu<sub>2</sub>O homojunction solar cells, *J. Phys. Chem. Lett.* (2010) 2666–2670.
- [7] J. Katayama, K. Ito, M. Matsuoka, J. Tamaki, Performance of Cu<sub>2</sub>O/ZnO solar cell prepared by two-step electrodeposition, *J. Appl. Electrochem.* (2004) 687.
- [8] N. Naka, K. Ito, M. Matsuoka, J. Tamaki, Thin films of single-crystal cuprous oxide grown from the melt, *Jpn. J. Appl. Phys.* (2005) 5096.
- [9] A. Mittiga, E. Salza, F. Sarto, M. Tucci, R. Vasanthi, Heterojunction solar cell with 2% efficiency based on a Cu<sub>2</sub>O substrate, *Appl. Phys. Lett.* (2006) 163502.
- [10] R. Brewer, H.A. Atwater, Rapid biaxial texture development during nucleation of MgO thin films during ion beam-assisted deposition, *Appl. Phys. Lett.* (2002) 3338.